

# Enabling Population-Based Architectures for Neural Combinatorial Optimization

Andoni Irazusta Garmendia, Josu Ceberio, Alexander Mendiburu,

University of the Basque Country (EHU),

Department of Computer Science and Artificial Intelligence, San Sebastian, Spain.

**Abstract**—Neural Combinatorial Optimization (NCO) has mostly focused on learning policies, typically neural networks, that operate on a single candidate solution at a time, either by constructing one from scratch or iteratively improving it. In contrast, decades of work in metaheuristics have shown that maintaining and evolving populations of solutions improves robustness and exploration, and often leads to stronger performance. To close this gap, we study how to make NCO explicitly population-based by learning policies that act on sets of candidate solutions. We first propose a simple taxonomy of “population awareness” levels and use it to highlight two key design challenges: (i) how to represent a whole population inside a neural network, and (ii) how to learn population dynamics that balance intensification (generating good solutions) and diversification (maintaining variety). We make these ideas concrete with two complementary tools: one that improves existing solutions using information shared across the whole population, and the other generates new candidate solutions that explicitly balance being high-quality with diversity. Experimental results on Maximum Cut and Maximum Independent Set indicate that incorporating population structure is advantageous for learned optimization methods and opens new connections between NCO and classical population-based search.<sup>1</sup>

**Index Terms**—Neural Combinatorial Optimization, Learning to Optimize, Population Methods, Reinforcement Learning.

## I. INTRODUCTION

**N**EURAL Combinatorial Optimization (NCO) [1], [2], [3] studies *learning-based* approaches for solving combinatorial optimization problems of different nature, such as routing [4], assignment [5], scheduling [6], or graph problems [7]. Instead of manually designing problem-specific heuristics, NCO trains parametric policies, typically neural networks, that either construct solutions step by step or improve existing solutions via learned local moves.

NCO is still far less mature than the rich body of classical heuristics and metaheuristics [8], [9], and has not yet consistently surpassed state-of-the-art methods in terms of solution quality and robustness across diverse benchmarks. Nonetheless, compared with classical methods (e.g., greedy construction, local search, simulated annealing, tabu search, or evolutionary algorithms) [8], NCO offers three benefits that are increasingly relevant at scale. First, it can automatically learn problem-specific guidance rules from data, for example, how to rank candidate moves, which neighborhoods to try first, or how to extend partial solutions [1], [2], [10]. Second, once

<sup>1</sup>This work has been submitted to the IEEE for possible publication. Copyright may be transferred without notice, after which this version may no longer be accessible.

trained, the resulting policy can be reused across many new instances with minimal additional computation or per-instance tuning [4], [11]. Third, NCO maps naturally to modern accelerators (GPUs), enabling batched inference and high-throughput evaluation of candidate moves or solutions [4], [11].

In practice, NCO and metaheuristics can coexist with different deployment profiles: metaheuristics are typically easier to prototype and broadly robust, whereas learned policies require more engineering and data but excel when rapid, repeated inference over many instances is needed [9], such as in online decision-making systems [12], real-time applications [13], or large-scale optimization pipelines [14].

Beyond the advantages outlined above, the development of NCO methods has largely mirrored the historical trajectory of heuristic and metaheuristic methods [8]. Early work adopted *Neural Constructive* (NC) policies [15], [3], [4], [11] that build solutions iteratively, adding one item at a time using a learned heuristic. This was later followed by *Neural Improvement* (NI) [16], [17], [7], [18], echoing classical local search, where a policy proposes local moves to improve a given solution. More recent efforts introduce tabu-like memory mechanisms [19], [20], [21], which track recent action histories to prevent getting stuck in local optima.

However, to the best of our knowledge, there is no prior work that learns a population-aware policy in an NCO framework. Instead, the most closely related lines of work fall into two categories: (i) *Deep Learning-assisted metaheuristics*, where learning parametrizes specific components of the metaheuristic while the population mechanics remain classical (e.g., learned crossover and selection [22], Genetic Algorithm initialization [23], or learning heuristics for Ant Colony Optimization [24], [25]), (ii) *Neural ensembles*, that train several different policies (or decoders) so that each one generates solutions in its own specialized way [26], [27]. These approaches can produce diverse solutions, but the policies do not interact with one another: there is no population-level coordination, and each policy works as an isolated individual.

Given the long-standing success of population-based metaheuristics in combinatorial optimization [8], [28], [25], and the strong improvements already demonstrated by neural constructive [11], [29] and neural improvement approaches [7], [18], extending NCO methods toward a neural population-based search paradigm represents a natural, highly promising and still underexplored direction. However, this extension raises several nontrivial challenges: how to process and evolve a population within a neural architecture; how to balance in-

tensification and diversification when the *operators* are neural networks; and how to train these systems efficiently, as the shift from single-solution optimization to population evolution introduces complex interactions that complicate the learning signal.

In this work, we take a first step in that direction by framing neural population-based search as the problem of learning *population operators* that act on sets of solutions rather than isolated individuals. We identify representation, coordination, and training as the core design dimensions, and instantiate them through two complementary components: i) a contextual improvement policy, a learned local search operator that uses a central memory to share information throughout the population, and (ii) a conditioned constructive policy, an operator that generates new solutions, using a steerable exploration weight to explicitly regulate the trade-off between solution quality and population diversity. Combining these components yields a population-based NCO framework (PB-NCO) that alternates memory-guided local search with diversity-aware *restarts*, where non-improving individuals are discarded and replaced by new candidates sampled from the conditioned constructive policy.

We assess the framework on Maximum Cut (MC) [30] and Maximum Independent Set (MIS) [31] across different graph families and problem sizes. The study includes performance and diversity analyses, as well as ablations that quantify the sensitivity of key components. We compare against classical population-based methods and leading neural baselines under matched time budgets. Overall, the proposed population-based methods achieve promising results that are competitive with these strong baselines.

The remainder of this paper is organized as follows. Section II reviews relevant background on NCO, including search settings, policy architectures, and learning paradigms. Section III introduces a taxonomy of different population-awareness levels and formalizes the main design challenges for neural population-based methods. Section IV presents our proposals, detailing the contextual neural improvement (cNI) and conditioned neural constructive (cNC) components and their integration into the complete framework PB-NCO. Section V describes the experimental setup and reports empirical results. Section VI discusses implications, limitations, and natural extensions of our approach, and Section VII concludes the paper. To facilitate reproducibility and cumulative progress, we release code, graph generators, and evaluation pipelines, including full training and evaluation configurations <sup>2</sup>.

## II. BACKGROUND

### A. Combinatorial Optimization

Let  $\mathcal{I}$  denote an instance of a combinatorial optimization problem with a feasible set  $\mathcal{S}(\mathcal{I})$  and an objective function  $f_{\mathcal{I}} : \mathcal{S}(\mathcal{I}) \rightarrow \mathbb{R}$ . Without loss of generality, we adopt the maximization convention (minimization problems can be handled by sign inversion). Each feasible configuration  $\mathbf{s} \in \mathcal{S}(\mathcal{I})$

represents a candidate solution, and the goal is to find one that maximizes the objective value:

$$\mathbf{s}^* \in \arg \max_{\mathbf{s} \in \mathcal{S}(\mathcal{I})} f_{\mathcal{I}}(\mathbf{s}). \quad (1)$$

### B. Neural Combinatorial Optimization

Neural Combinatorial Optimization (NCO) [1], [2], [3] refers to methods that solve combinatorial problems by learning a policy directly from data. Formally, we consider a state space  $\mathcal{X}$  and, for each state  $x \in \mathcal{X}$ , a set of feasible actions  $\mathcal{A}(x)$ . A policy  $\pi_{\theta}$  with parameters  $\theta$  maps each state to a probability distribution over actions  $\pi_{\theta} : \mathcal{X} \rightarrow \mathcal{A}$ .

NCO typically follows a *train–inference* scheme: in the training phase,  $\pi_{\theta}$  is optimized offline on a distribution of problem instances to discover decision patterns that lead to high-quality solutions; at inference time, the same policy is applied to new unseen instances, requiring only forward passes of the network and thus incurring a relatively low computational cost compared to training.

In NCO, the search process is modeled as a sequence of decisions. At each step  $t$ , the policy  $\pi_{\theta}$  observes the current state  $x_t \in \mathcal{X}$ , which encodes both the problem instance  $\mathcal{I}$  and its current search context, and selects an action  $a_t \in \mathcal{A}(x_t)$ . This interaction produces a trajectory

$$\tau = (x_0, a_0, x_1, a_1, \dots, a_T, x_T).$$

Two settings are typically distinguished. In the **Constructive setting**, the state  $x_t$  encodes a partial solution,  $x_t = (\mathcal{I}, \text{partial } s_t)$ , typically starting from an empty solution. At each step, the policy selects an action that adds one component, and the process continues until a complete feasible solution  $s_T \in \mathcal{S}(\mathcal{I})$  is obtained. In the **Improvement setting**, the state contains a complete feasible solution,  $x_t = (\mathcal{I}, s_t)$ , and actions correspond to local modifications within a neighborhood  $\mathcal{N}(s_t) \subseteq \mathcal{S}(\mathcal{I})$  that aim to improve it. These moves are applied iteratively until a stopping criterion is met (e.g., no further improvement, iteration limit, or time budget).

In both settings, the policy  $\pi_{\theta}$  must encode the combinatorial structure of the instance together with the current search state and map this representation to an action. The concrete way this is implemented is detailed in the following subsection.

### C. Model Architecture

Most NCO policy architectures follow a two-stage design (see Fig. 1): (i) an *encoder* that receives the instance features together with the current state of the search and produces a representation in the latent space, and (ii) a *decoder* that uses these representations to select an action specifying how to construct or modify the solution.

The encoder typically operates on graph-structured inputs, as many combinatorial optimization problems can be naturally represented as a graph  $\mathcal{G} = (\mathcal{V}, \mathcal{E})$  [13], where nodes denote items or decisions and edges encode pairwise relations (e.g., distances, conflicts, compatibilities). Each node and each edge is described by two types of features: *static* features, which encode instance-specific information such as weights or costs

<sup>2</sup>Code will be made publicly available upon acceptance.

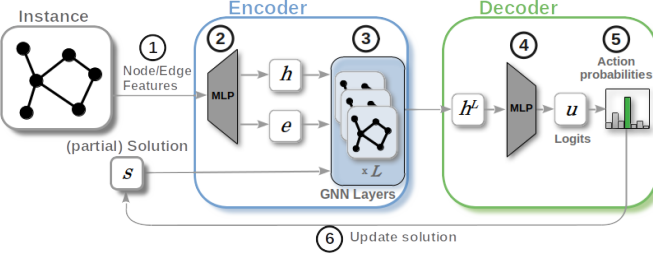


Fig. 1. High-level encoder-decoder architecture used in Neural Combinatorial Optimization. First (1) graph features (node/edge) are extracted, the encoder then produces node embeddings  $h$  and edge embeddings  $e$ , projecting features to a  $d$ -dimensional space (2), and these are processed by a GNN through  $L$  layers (3). The last layer embeddings are then used by a decoder (4) to produce action logits, that form action probabilities (5) that modify the current solution (6).

and do not change throughout the search process, and *dynamic* features, which encode the current search state, and are updated as the search progresses, for example, to indicate the current (partial or complete) solution, the role of a node in the neighborhood of the current candidate, or other problem-specific indicators.

All static and dynamic node and edge features (step 1 in Fig. 1) are first projected into a  $d$ -dimensional embedding space, yielding initial node embeddings  $h_i^{(0)} \in \mathbb{R}^d$  for each node  $i \in \mathcal{V}$  and, similarly, initial edge embeddings  $e_{ij}^{(0)} \in \mathbb{R}^d$  for each edge  $(i, j) \in \mathcal{E}$  (step 2). These embeddings are then processed by a Graph Neural Network (GNN) [13] for  $L$  message-passing layers (step 3)<sup>3</sup>, producing final node embeddings  $h_i^{(L)} \in \mathbb{R}^d$ ,  $i \in \mathcal{V}$ , which are subsequently inputted to the decoder.

The decoder (typically a multi-layer perceptron) produces one scalar action logit for each feasible action. Depending on the problem and the search setting (constructive or improvement), these actions are defined either on nodes or on edges. For node-based actions, it maps each node embedding  $h_i^{(L)} \in \mathbb{R}^d$  to a logit  $u_i \in \mathbb{R}$  (step 4), representing the relative preference for selecting node  $i$ . For edge-based actions (e.g., pairwise operators), we first form an edge embedding by concatenating the endpoint embeddings,  $h_{ij} = [h_i^{(L)}; h_j^{(L)}] \in \mathbb{R}^{2d}$ , and apply the same decoder to obtain an edge logit  $u_{ij} \in \mathbb{R}$ . A softmax over the feasible action set  $\mathcal{A}(x_t)$  then converts these logits into a probability distribution over actions (step 5):

$$\pi_\theta(a_t = a | x_t) = \frac{\exp(u_a)}{\sum_{a' \in \mathcal{A}(x_t)} \exp(u_{a'})}, \quad (2)$$

from which an action is sampled or greedily selected to update the current solution (step 6).

For a comprehensive overview of GNN-based architectures for combinatorial optimization, including message passing and action decoding mechanisms, we refer the reader to Cappart et al. [13].

<sup>3</sup>GNNs are a standard choice for the encoder because they respect the symmetries of combinatorial problems (permutation equivariance with respect to node order) and allow the same architecture to operate on graphs of varying sizes.

#### D. Policy Learning

The original NCO approaches [3] were developed within a Reinforcement Learning (RL) [32] framework. Although earlier [15] and subsequent studies [1] have explored supervised and unsupervised training schemes, RL, and in particular policy-gradient methods [2], remain the predominant learning paradigm in the NCO literature.

In this setting, the policy  $\pi_\theta$  is executed on many instances, receives feedback in the form of rewards, and its parameters  $\theta$  are updated so as to maximize the expected return, increasing the probability of actions that yielded higher returns. Formally, let  $r_t$  denote the reward given at decision step  $t$ , and define the discounted return from time  $t$  as

$$\hat{G}_t = \sum_{t'=t}^T \gamma^{t'-t} r_{t'}, \quad \gamma \in [0, 1], \quad (3)$$

where the discount factor  $\gamma$  can be used to emphasize earlier steps and reduce variance in long decision-trajectories.

In the policy-gradient (PG) scheme, the objective function is

$$\mathcal{J}_{\text{PG}}(\theta) = \mathbb{E}_{\tau \sim \pi_\theta} \left[ \sum_{t=0}^T \log \pi_\theta(a_t | x_t) A_t \right], \quad (4)$$

where  $A_t = \hat{G}_t - B(x_t)$  is the *advantage*, measuring how much better an action performs compared to an action-independent baseline  $B(x_t)$ . The baseline acts as a control variate: it centers the returns and reduces gradient variance, without changing which policy is optimal. Intuitively, Equation (4) increases the probability of actions with positive  $A_t$  and decreases it for negative  $A_t$ . This formulation applies to both the constructive and improvement settings; only the definition of the reward  $r_t$  in Equation (3) differs.

In the *constructive setting*, rewards are only given once a complete solution ( $s_T$ ) is constructed: all intermediate rewards are zero and the terminal reward equals the objective:

$$r_t = 0 \quad (t < T), \quad r_T = f_{\mathcal{I}}(s_T). \quad (5)$$

In this purely terminal case,  $\gamma$  has no effect.

In the *improvement setting*, the reward is defined per improvement step as the immediate gain in objective value:

$$r_t = f_{\mathcal{I}}(s_{t+1}) - f_{\mathcal{I}}(s_t) \quad (6)$$

Here,  $\gamma = 1$  yields undiscounted finite-horizon optimization;  $0 < \gamma < 1$  progressively downweights later improvements (more myopic), and  $\gamma = 0$  reduces updates to purely one-step improvement.

Once the reward values are computed, policy parameters  $\theta$  are updated using stochastic gradient ascent over the objective  $\mathcal{J}_{\text{PG}}$ :

$$\theta \leftarrow \theta + \eta \widehat{\nabla_\theta \mathcal{J}_{\text{PG}}} \quad (7)$$

where  $\eta > 0$  is the learning rate and  $\widehat{\nabla_\theta \mathcal{J}_{\text{PG}}}$  denotes the gradient estimate computed from the sampled trajectories.

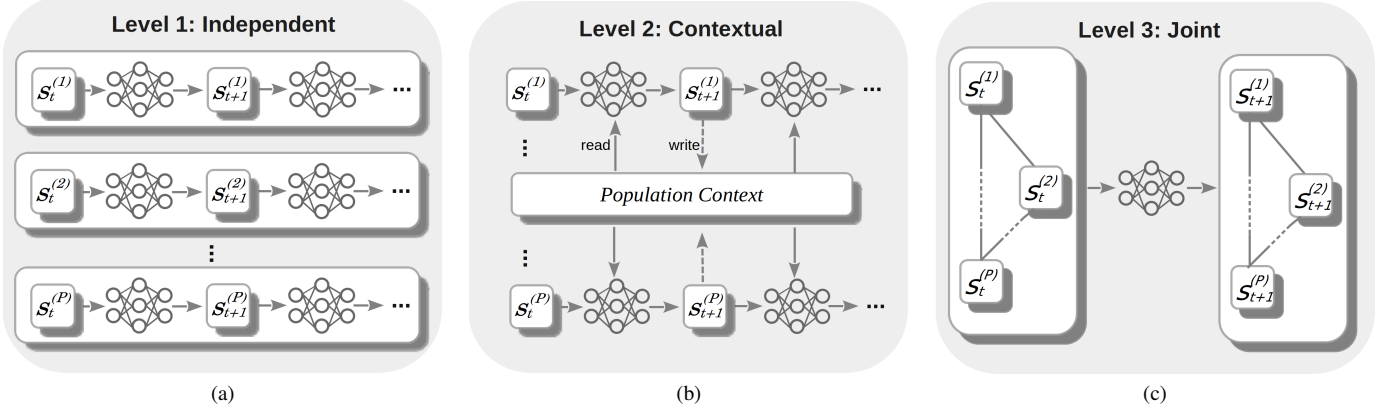


Fig. 2. **Three levels of population awareness in neural population-based methods.** (a) **Independent:** Each solution  $s_t^{(i)}$  is improved in isolation. The policy is applied in parallel to multiple starting points, but there is no exchange of information between runs (equivalent to multi-start NCO). (b) **Contextual:** Each solution is updated based on its own state and an external context signal. This context can be global (e.g., a shared memory) or directed (e.g., peer-to-peer communication from specific neighbors). (c) **Joint:** The model reasons jointly about multiple solutions at once, allowing explicit pairwise or group interactions across the population.

### III. TAXONOMY AND DESIGN CHALLENGES FOR NEURAL POPULATION-BASED METHODS

As discussed in Section I, most existing NCO methods operate on a single solution at a time. Extending them to a population-based framework raises new questions about how neural architectures could effectively represent and evolve a *set* of solutions.

We denote by  $\mathcal{P}_t = \{s_t^{(i)}\}_{i=1}^P$  a population of  $P$  candidate solutions at iteration  $t$  for an instance  $\mathcal{I}$ . A neural population-based method can then be viewed as a learned operator

$$F_\theta : (\mathcal{I}, \mathcal{P}_t) \mapsto \mathcal{P}_{t+1}, \quad (8)$$

whose goal is to transform  $\mathcal{P}_t$  into a new population  $\mathcal{P}_{t+1}$  such that solution quality improves over time.

To reason about potential population-based extensions of NCO, we introduce a simple taxonomy that classifies how much population information is exposed to each decision (see Fig. 2), ranging from no population awareness to full joint reasoning over multiple individuals. This framework allows us to interpret existing single-solution NCO methods as a degenerate, population-unaware case, and to use the richer levels to motivate the specific design choices behind our cNI and cNC components.

- **Level 1: Independent.** The policy evolves each solution  $s_t$  based solely on its own trajectory, with no information exchanged across runs. In practice, the  $P$  solutions are treated as a batch: the same improvement policy is applied in parallel from multiple random starts, and the model only sees  $P$  isolated trajectories, as in standard single-trajectory NCO methods [1], [3], [4]. Formally, the policy factorizes over solutions as

$$x_t^{(i)} = (\mathcal{I}, s_t^{(i)}), \quad a_t^{(i)} \sim \pi_\theta(a | x_t^{(i)}), \quad (9)$$

and the next population  $\mathcal{P}_{t+1}$  is obtained by applying the underlying NCO update rule to each solution independently.

- **Level 2: Contextual.** The policy acts locally on each individual, but it is conditioned on an external context

signal that depends on the rest of the population. The search state is

$$x_t^{(i)} = (\mathcal{I}, s_t^{(i)}, c_t^{(i)}), \quad (10)$$

where

$$c_t^{(i)} = C_\theta(s_t^{(i)}, \mathcal{P}_t) \quad (11)$$

is a population-derived context vector for individual  $i$ . The mapping  $C_\theta$  can be any function of the population and the focal individual, such as a shared summary over all solutions, a  $k$ -nearest-neighbor descriptor, or an aggregation over neighbors in a similarity graph.

- **Level 3: Joint.** In the richest form of population awareness, the policy processes several solutions in a single joint state

$$X_t = (x_t^{(1)}, \dots, x_t^{(P')}), \quad x_t^{(i)} = (\mathcal{I}, s_t^{(i)}), \quad (12)$$

for some subset  $\mathcal{P}' = \{s_t^{(i)}\}_{i=1}^{P'}$  of the population (e.g., the whole population or a selected reference set). Internal layers of the model explicitly mix information across the components of  $X_t$ , so that each decision can depend on the state of several solutions. The policy either produces a single action:  $a_t \sim \pi_\theta(\cdot | X_t)$ , or a joint action vector  $A_t = (a_t^{(1)}, \dots, a_t^{(P')}) \sim \Pi_\theta(\cdot | X_t)$  that involve several candidates.

The independent setting (Level 1) is simple and scalable: most existing single-trajectory NCO architectures, both constructive and improvement [1], [4], [16], [20], already fall into this category and can be run in a population mode by treating  $P$  solutions as a batch with little or no modification. However, this regime misses key advantages of population methods: individuals do not exchange information, search effort cannot be adaptively reallocated across trajectories, and there is no explicit mechanism to maintain or exploit diversity in the population. The richer Levels 2 and 3 are closer in spirit to classical population metaheuristics, but they introduce additional design challenges and, to the best of our knowledge,

remain largely unexplored in NCO. In what follows, we highlight three of the most important challenges.

**Population representation.** As mentioned before, by a population we mean a set of candidate solutions that are considered together during the search. This set can have variable size  $P$ , and different individuals may carry very different amounts of useful information (e.g., some are high-quality elites, others are diverse outliers).

Contextual and joint architectures (Levels 2 and 3) must therefore build an internal *representation* of this population that: (i) can handle variable population sizes  $P$  without changing the model structure; (ii) is invariant to the order in which individuals are listed (permutation symmetry), since the population is a set and not a sequence; and (iii) preserves enough information about the population to support good subsequent decisions, while keeping memory and computation costs manageable.

At Level 2, the key challenge is to compress the whole population into per-individual context vectors  $c_t^{(i)}$  that are both informative and cheap to compute. The mapping  $C_\theta(s_t^{(i)}, \mathcal{P}_t)$  in Eq. (11) does exactly this: for each focal solution  $s_t^{(i)}$ , it looks at the population  $\mathcal{P}_t$  and produces a short summary  $c_t^{(i)}$  that encodes relevant information about the population from the perspective of solution  $i$ . Designing  $C_\theta$  means deciding which other solutions each individual can “see” (e.g., elites, diverse outliers, or  $k$  nearest neighbors) and how to aggregate them into a fixed-size vector; if the summary is too coarse, the context is uninformative, whereas detailed summaries become expensive as problem or population size grows.

At Level 3, the population can be treated simply as a set (no explicit pairwise structure) or can be modeled with richer interactions between solutions. In the latter case, one must also decide how expressive these interactions should be (e.g., fully dense vs. sparse neighborhoods) while keeping the cost manageable. Ideally, the representation should be robust to permutations and varying population size  $P$ , but achieving this is non-trivial: it requires mapping a variable-size collection of variable-size solutions to a fixed number of embeddings without discarding too much information.

#### Control structure and learning objective.

Population-based search involves two kinds of decisions: (i) *local* decisions on individual solutions (e.g., which move to apply next), and (ii) *global* decisions about the population as a whole (e.g., which trajectories to restart, which solutions to keep, or how to distribute computation across individuals).

In a population-based RL setting, one could either define the objective separately for each individual solution or define a single objective for the population as a whole (e.g., based on the best or average solution quality). In the latter case, a single global scalar objective aggregates the effects of many local and global decisions made by different individuals over time, which leads to a credit-assignment problem, i.e., it becomes unclear which specific decisions were responsible for a good or bad outcome.

At Level 2, control remains mostly local, but each decision is modulated by a context derived from the population. Here, the challenge is to design learning signals that encourage the

policy to exploit this population context, rather than ignoring it and reverting to purely single-solution behavior.

At Level 3, a single network can update many individuals based on their joint state, and the reward depends on the combined outcome of all of them. In this regime, naïve global rewards provide very weak guidance, because each gradient step reflects many coordinated decisions at once. A practical way to mitigate this could be to decompose the population update into a sequence of smaller decisions (for example, updating one individual or subset at a time), so that more informative intermediate feedback can be provided and credit can be assigned more precisely.

**Maintaining diversity under learning.** A main motivation for using a population is to explore multiple regions of the search space in parallel. Yet, when a single neural policy is shared across all individuals and trained with a common RL objective that maximizes expected return, it tends to become confident and almost deterministic. In a population setting, this drives all individuals toward similar behaviors and the same basin of attraction, effectively wasting the population. Preventing this collapse requires explicit diversity mechanisms, acting either on the solutions (e.g., rewarding novelty or penalizing near-duplicates), on the behavior (e.g., assigning different roles or objectives to different individuals), or on the stochasticity of the policy (e.g., maintaining sufficient entropy).

In the next section, we address these challenges with concrete design choices that lead to a population-based neural architecture for combinatorial optimization.

## IV. A POPULATION-BASED NEURAL ARCHITECTURE

Building on the population awareness levels and the challenges outlined in Section III, we propose two population-based components:

- a *contextual Neural Improvement* (**cNI**) method (Level 2), designed to *improve* existing solutions by performing learned local search on each individual while reading and updating a central population memory; and
- a *conditioned Neural Constructive* (**cNC**) method (Level 3), designed to *generate* new solutions that are high-quality yet diverse with respect to a conditioning set of solutions.

The following subsections detail the two main components of our approach. We first present cNI, describing its interaction with the shared memory and its learning dynamics. We then introduce cNC, focusing on how it trades off solution quality and diversity, as well as its training scheme. Finally, we explain how these components are combined at inference time to form a more powerful, unified population-based framework, which we refer to as Population-Based Neural Combinatorial Optimization (**PB-NCO**).

### A. Contextual Neural Improvement Policy (Level 2)

In the improvement setting, the policy  $\pi_{\text{cNI}}^4$  conditions on both the instance and the current candidate solution  $s_t^{(i)}$ , and proposes a local modification (see Section II-B). Applied

<sup>4</sup>For notational convenience, we omit the parameter vector  $\theta$ .

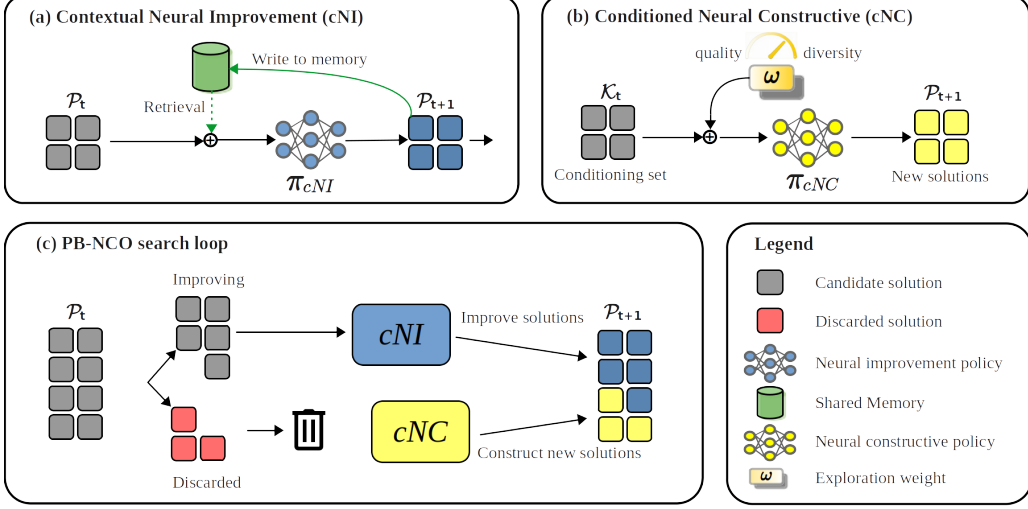


Fig. 3. **Overview of the proposed population-based NCO frameworks.** (a) A contextual neural improvement policy (cNI) applies learned local moves to each solution, using information retrieved from a shared population memory of visited candidates. (b) A conditioned neural constructive policy (cNC) samples new candidates given a conditioning set of solutions  $\mathcal{K}$  and an exploration weight  $\omega$ , which controls the trade-off between solution quality and diversity. (c) PB-NCO combines both components in a population loop, alternating cNI-driven improvement of existing solutions with cNC-driven restarts.

independently to a batch of candidates, this yields a Level 1 method:  $P$  isolated improvement trajectories with no information exchange. In contrast, we introduce a *contextual* neural improvement policy (Level 2) that exploits a shared memory that provides a population-context.

Concretely, a central *memory*  $\mathcal{M}_t$  stores all solutions visited by the population. At each step, and for every solution, the policy retrieves from  $\mathcal{M}_t$  a compact descriptor that summarizes the most relevant historical information for its current state. After using this information to propose a modification, the resulting solution is written back into memory (see Fig. 3a). This defines a simple read–write interaction pattern: individuals query the accumulated population history to guide their next move and, in turn, update that history for future queries.

This retrieval step is implemented as a  $k$ -nearest-neighbors (k-NN) query in solution space [20], defined by a problem-specific distance function  $d(\cdot, \cdot)$ . Given the current solution  $s_t^{(i)}$ , we select its  $k$  nearest neighbors  $\mathcal{N}_k(s_t^{(i)}) = \{s^{(j)} \in \mathcal{M}_t : j \in \mathcal{I}_k\}$ , where  $\mathcal{I}_k$  indexes the  $k$  entries in  $\mathcal{M}_t$  with smallest distance  $d(s_t^{(i)}, s^{(j)})$ . These neighbors are aggregated into a fixed-size descriptor  $z_t^{(i)} = \sum_{j \in \mathcal{I}_k} \alpha_j s^{(j)}$ , where the weights  $\alpha_j$  decay linearly with distance so that closer neighbors contribute more. Concretely, we compute distances  $d_j = d(s_t^{(i)}, s^{(j)})$ , min–max normalize them to  $\tilde{d}_j = (d_j - d_{\min}) / (d_{\max} - d_{\min} + \epsilon)$ , invert them as  $w_j = 1 - \tilde{d}_j$  so that the closest neighbor attains weight  $w_j = 1$  and the farthest  $w_j = 0$ , and finally normalize to  $\alpha_j = w_j / \sum_{\ell \in \mathcal{I}_k} w_\ell$ .

The resulting descriptor, denoted  $z_t$  for brevity, is injected by augmenting the dynamic features of the current search state. Since  $z_t \in \mathbb{R}^{|\mathcal{V}|}$  is a solution-space vector, we use it as a *per-node* channel. For node-based representations, we append  $z_{t,u}$  to node  $u$ 's features:  $\tilde{h}_u = [h_u; z_{t,u}]$  for all nodes  $u \in \mathcal{V}$ . For edge-based representations, we instead concatenate an edge-wise scalar  $z_{t,uv}$  to the dynamic edge features, obtaining  $\tilde{e}_{uv} = [e_{uv}; z_{t,uv}]$  for all edges  $(u, v) \in \mathcal{E}$ .

To ensure bounded memory use, the shared memory  $\mathcal{M}_t$

is maintained with a fixed capacity  $M_{\max}$ . When this limit is reached, newly added solutions remove the oldest entries following a first-in–first-out policy.

To guide policy learning on top of this memory-augmented architecture, we define the per-step reward as the sum of two complementary components: an *objective reward* that encourages genuine progress in solution quality and a *repetition penalty* that discourages revisiting already explored solutions.

a) *Objective reward*: Rather than rewarding every small local gain as in Eq. 6, we use the best solution found in each trajectory as a moving reference. Let

$$B_t^{(i)} = \max\{f(s_\tau^{(i)}) : 0 \leq \tau \leq t\} \quad (13)$$

be the best objective value achieved up to iteration  $t$ , and let  $s_{t+1}^{(i)}$  denote the post-action solution. The objective reward is then the non-negative improvement over this reference:

$$R_{\text{obj},t}^{(i)} = \max\{f(s_{t+1}^{(i)}) - B_t^{(i)}, 0\} \quad (14)$$

This choice makes the cumulative reward along a trajectory equal to the net improvement in  $f$ , which tolerates occasional worsening moves on the path to a better solution.

b) *Repetition penalty*: To prevent cycling and increase exploration, we include a repetition penalty that activates when an individual revisits an already stored solution in the shared memory:

$$R_{\text{rep},t}^{(i)} = \begin{cases} -1, & \text{if } s_{t+1}^{(i)} \in \mathcal{M}_t, \\ 0, & \text{otherwise.} \end{cases} \quad (15)$$

We deliberately use a binary penalty rather than a distance- or diversity-based term. Explicitly maximizing diversity in a local improvement setting, would encourage moves that push trajectories far away from the visited solutions, potentially bypassing nearby improvements. In contrast, the binary penalty simply discourages revisiting previously seen solutions while allowing focused exploration in the surrounding neighborhood. In Section IV-B, we show that in a constructive setting, where

solutions are generated from scratch, distance-based diversity penalties become more appropriate.

The total per-step reward is

$$R_{cNI,t}^{(i)} = R_{\text{obj},t}^{(i)} + w_{\text{rep}} R_{\text{rep},t}^{(i)} \quad (16)$$

with a tunable weight  $w_{\text{rep}} \geq 0$  that controls the strength of the repetition penalty.

### B. Conditioned Neural Constructive Policy (Level 3)

The second proposed component is a Level 3 method: a *conditioned neural constructive* (cNC) policy designed to generate new candidates by trading off solution quality against distance from a reference set  $\mathcal{K}$  (see Fig. 3b). In population-based search, quality and diversity form an intrinsically bi-objective goal: pushing solely for quality causes the population to converge prematurely to a small set of nearly identical elites, while forcing diversity alone harms objective performance. To manage this, we draw inspiration from Conditioned Networks [33], originally proposed for multi-objective RL [34], and expose this trade-off directly to the network via explicit conditioning variables.

We instantiate this idea as a policy  $\pi_{\text{cNC}}$  that extends the standard constructive architecture (Section II-B) with two additional inputs: a *conditioning set*  $\mathcal{K}$  and an *exploration weight*  $\omega$ .

At step  $t$ , the policy observes a reference set of solutions  $\mathcal{K}_t = \{s^{(1)}, \dots, s^{(|\mathcal{K}_t|)}\}$  (e.g., the current population or a subset of elites), which indicates which regions of the search space have already been explored. To encode this, we fix a maximum conditioning size  $K_{\text{max}}$  and augment the graph features with  $K_{\text{max}}$  additional channels. As a practical example, for node-based encodings, each solution  $s^{(k)}$  is mapped to a binary indicator vector

$$m_u^{(k)} \in \{0, 1\}, \quad u \in \mathcal{V}, \quad (17)$$

specifying whether node  $u$  participates in  $s^{(k)}$ . The augmented node features become

$$\tilde{h}_u = [h_u; m_u^{(1)}; \dots; m_u^{(K_{\text{max}})}], \quad (18)$$

where unused channels are zero-padded if  $|\mathcal{K}_t| < K_{\text{max}}$ . For edge-based representations, the same would be done for edge features.

To explicitly control this behavior, we introduce a scalar exploration weight  $\omega \in [0, 1]$ , which is broadcast as an additional node feature:

$$\tilde{h}_u \leftarrow [\tilde{h}_u; \omega], \quad u \in \mathcal{V}. \quad (19)$$

When  $\omega \approx 0$ , the policy is encouraged to exploit and produce high-quality solutions with minimal regard to  $\mathcal{K}_t$ . Conversely, when  $\omega \approx 1$ , it prioritizes diversity by generating solutions that are structurally distinct from the reference set. Intermediate values interpolate between these behaviors, encouraging solutions that balance quality and novelty.

*a) Training Objective:* To enable the policy to generalize across the full spectrum of the quality–diversity trade-off, we employ a randomized training scheme. For each problem instance in a training batch, we first generate a synthetic conditioning set  $\mathcal{K}_t$  (by random initialization) and sample a scalar exploration weight  $\omega$ . The policy  $\pi_{\text{cNC}}$  then constructs a candidate solution  $s'$ , conditioned on both the problem instance and the tuple  $(\mathcal{K}_t, \omega)$ .

The training signal is derived from a scalar reward  $R_{\text{cNC}}$  that weights the objective maximization and repulsion from the conditioning set:

$$R_{\text{cNC},t}(s') = (1 - \omega) f(s') + \omega \cdot \frac{1}{|\mathcal{K}_t|} \sum_{m \in \mathcal{K}_t} d(s', m), \quad (20)$$

Here,  $f(s')$  denotes the objective value, and  $d(s', m)$  represents the distance between the new solution  $s'$  and a reference solution  $m$ .

During training, we sample the exploration weight from a symmetric Beta distribution,  $\omega \sim \text{Beta}(\alpha, \beta)$  with  $\alpha = \beta = 0.2$ . This distribution is bi-modal, concentrating probability mass near 0 and 1. This forces the network to master the distinct tasks of pure exploitation (quality maximization) and pure exploration (diversity maximization). For the policy-gradient update (Eq. 4), the advantage  $A_t$  is computed using a baseline  $B(x_t)$  given by the mean reward of multiple candidate solutions  $s'$  generated for the same instance.

*b) Inference and Integration:* In this paper we use cNC in three complementary ways. First, as a *greedy constructive* heuristic: we set  $\omega = 0$  and perform a single construction per instance, so that cNC behaves as a fast, quality-focused method. Second, as a *population-based generator*: we maintain an explicit population and, at each iteration, take the current population as the reference set  $\mathcal{K}_t$ . We then apply cNC to sample new candidates that will define the new population, while varying  $\omega$  over time according to a defined schedule to interpolate between exploitation and exploration. Third, cNC acts as a *restart operator* within our full PB-NCO framework, as detailed in the following subsection.

### C. PB-NCO search scheme

PB-NCO combines the contextual improvement policy (cNI) and the conditioned constructive policy (cNC) within a unified population-based search loop. As illustrated in Fig. 3c, each individual in the population repeatedly alternates between two phases: (i) *local improvement* driven by cNI, and (ii) *restart and diversification* guided by cNC.

During the improvement phase, cNI proposes local modifications to refine the current solution while using the shared memory to avoid immediate cycling. This mechanism steadily pushes individuals toward high-quality regions of the search space. However, improvement alone cannot ensure broad exploration: once an individual stops progressing, continuing to apply cNI yields little benefit.

To address this, PB-NCO introduces a learned restart mechanism. When an individual’s trajectory becomes stagnant (detected via a patience counter) its current solution is discarded and replaced by a new candidate generated by cNC. The cNC

**Algorithm 1** Inference Pipeline

```

1: Input: instance  $\mathcal{I}$ ; trained improvement policy  $\pi_{\text{cNI}}$ ; trained
   conditioned constructor  $\pi_{\text{cNC}}$ ; population size  $P$ ; horizon  $T_{\max}$ ;
   patience  $N_{\text{pat}}$ ; initial exploration weight  $\omega_{\text{start}}$ ; cooling factor  $\phi$ 
2: Initialize:
3:  $\mathcal{M}_0 \leftarrow \emptyset$  {shared memory}
4:  $s^* \leftarrow \emptyset$ ,  $f(s^*) \leftarrow -\infty$  {best-so-far}
5: for  $i \in \{1, \dots, P\}$  do
6:    $s_0^{(i)} \leftarrow \text{Init}(\mathcal{I})$  {feasible initialization}
7:    $c^{(i)} \leftarrow 0$  {consecutive non-improving steps}
8:    $B_0^{(i)} \leftarrow f(s_0^{(i)})$  {per-individual best-so-far value}
9:    $\mathcal{M}_0 \leftarrow \text{UpdateMemory}(\mathcal{M}_0, s_0^{(i)})$ 
10: end for
11: for  $t = 0$  to  $T_{\max} - 1$  do
12:   for  $i \in \{1, \dots, P\}$  do
13:     if  $c^{(i)} \geq N_{\text{pat}}$  then
14:        $\omega \leftarrow \omega_{\text{start}} \left(1 - \frac{t}{T_{\max}}\right)^\phi$  {budget-aware schedule}
15:        $\mathcal{K}_t \leftarrow \text{SelectK}(\mathcal{M}_t)$  {top-quality / most-novel}
16:        $s_{t+1}^{(i)} \leftarrow \pi_{\text{cNC}}(\mathcal{I}, \mathcal{K}_t, \omega)$  {construct new solution}
17:        $c^{(i)} \leftarrow 0$ ,  $B_{t+1}^{(i)} \leftarrow \max\{B_t^{(i)}, f(s_{t+1}^{(i)})\}$ 
18:     else
19:        $s_{t+1}^{(i)} \leftarrow \pi_{\text{cNI}}(\mathcal{I}, s_t^{(i)}, \mathcal{M}_t)$  {perform local move}
20:       if  $f(s_{t+1}^{(i)}) > B_t^{(i)}$  then
21:          $c^{(i)} \leftarrow 0$ ,  $B_{t+1}^{(i)} \leftarrow f(s_{t+1}^{(i)})$ 
22:       else
23:          $c^{(i)} \leftarrow c^{(i)} + 1$ ,  $B_{t+1}^{(i)} \leftarrow B_t^{(i)}$ 
24:       end if
25:     end if
26:    $\mathcal{M}_{t+1} \leftarrow \text{UpdateMemory}(\mathcal{M}_t, s_{t+1}^{(i)})$ 
27:   if  $f(s_{t+1}^{(i)}) > f(s^*)$  then
28:      $s^* \leftarrow s_{t+1}^{(i)}$  {update best-so-far}
29:   end if
30: end for
31: end for
32: Output:  $s^*$ 

```

receives a conditioning set  $\mathcal{K}_t$  extracted from the population or from memory, and an exploration weight  $\omega$  to generate the new candidate.

Algorithm 1 summarizes the full inference pipeline. The algorithm takes as input an instance  $\mathcal{I}$ , trained policies  $\pi_{\text{cNI}}$  and  $\pi_{\text{cNC}}$ , and several runtime parameters: population size  $P$ , iteration budget  $T_{\max}$ , patience threshold  $N_{\text{pat}}$ , and an exploration-weight schedule specified by  $\omega_{\text{start}}$  and cooling exponent  $\phi$ . PB-NCO begins by generating  $P$  feasible starting solutions, either randomly or using a highly exploitative call to cNC, and inserting them into the shared memory.

The main loop (lines 12–32) then iterates over all individuals. As long as an individual continues to improve, cNI generates local moves conditioned on the memory. When no improvement has been observed for  $N_{\text{pat}}$  consecutive steps, the individual is restarted: a conditioning set  $\mathcal{K}_t$  is selected, a budget-aware exploration weight  $\omega$  is computed, and cNC constructs a new solution conditioned on  $(\mathcal{I}, \mathcal{K}_t, \omega)$ . Each new solution, whether obtained through improvement or restart, is written to the shared memory, and the global best solution  $s^*$  is updated whenever a better objective value is encountered.

The algorithm outputs this best solution at termination.<sup>5</sup>

**V. EXPERIMENTS**

In this section we evaluate the proposed population-based framework and the involved components: the contextual Neural Improvement policy (cNI), the conditioned Neural Constructive policy (cNC), and their combination PB-NCO. We study cNI as a standalone improvement method, cNC both as a single-pass greedy constructive heuristic (cNC<sub>greedy</sub>) and as a population-based generator (cNC<sub>pop</sub>), and PB-NCO as the full intensification–diversification framework described in Section IV-C. The following analysis focuses on four aspects: (i) *performance* under equal time budgets against exact solvers, classical heuristics and metaheuristics, specialized algorithms, and learning-based baselines, reporting best-so-far tables and anytime curves; (ii) *diversification*, analyzing how population-level coordination affects exploration and diversity throughout the search; (iii) *ablations and sensitivity*, assessing the impact of key design choices such as shared memory, learned restarts, exploration-weight scheduling, restart patience, and population size; and (iv) the *bi-objective training behavior* of cNC, viewed as a quality–diversity policy.

We begin by specifying the tackled problems and the common experimental setting.

TABLE I  
MC AND MIS PERFORMANCE TABLE. THE BEST OVERALL RESULTS ARE HIGHLIGHTED IN BOLD. \*THE BEST PERFORMING BASELINE IS USED TO COMPUTE THE RATIOS.

	Method	Type	ER700-800			RB800-1200		
			Obj.	Ratio	Time	Obj.	Ratio	Time
Maximum Cut (MC)	GUROBI	Exact	23420.17	0.966	1.00m	20290.08	0.643	1.00m
	Greedy	Heuristic	23774.79	0.980	0.03 s	30619.32	0.971	0.04 s
	GA	Metaheuristic	24211.64	0.999	1.00m	31542.89	1.000	1.00m
	PSO	Metaheuristic	24201.78	0.999	1.00m	*31544.80	1.000	1.00m
	BURER	Specialized	*24235.93	1.000	1.00m	29791.52	0.944	1.00m
	S2V-DQN	RL / NC	21581.79	0.890	10.1 s	22014.93	0.698	13.4 s
FlowNet	FlowNet	UL / NC	21727.19	0.896	1.14 s	23410.60	0.742	2.97 s
	ECO-DQN	RL / NI	24114.06	0.994	2.10m	29638.78	0.940	3.00m
	ANYCSP	RL / NI	24211.00	0.999	35.7m	31544.76	1.000	42.4m
	MARCO	RL / NI	24205.97	0.998	1.67m	29780.71	0.944	2.75m
	cNC <sub>greedy</sub>	RL / NC	23968.41	0.989	0.01 s	31201.02	0.989	0.02 s
Maximum Independent Set (MIS)	cNC <sub>pop</sub>	RL / NC	24225.75	1.000	1.00m	31545.60	1.000	1.00m
	cNI	RL / NI	24221.72	0.999	1.00m	31544.85	1.000	1.00m
	PB-NCO	RL / NI+NC	<b>24266.33</b>	<b>1.001</b>	1.00m	<b>31547.50</b>	<b>1.000</b>	1.00m
	GUROBI	Exact	43.47	0.966	1.00m	40.90	0.947	1.00m
	Greedy	Heuristic	38.85	0.863	0.05 s	37.78	0.875	0.06 s
DGL	GA	Metaheuristic	43.97	0.977	1.00m	41.39	0.959	1.00m
	PSO	Metaheuristic	43.69	0.971	1.00m	41.19	0.955	1.00m
	KAMIS	Specialized	*44.98	1.000	1.00m	* <b>43.15</b>	<b>1.000</b>	1.00m
	INTEL	SL / Hybrid	38.71	0.861	11.0 s	32.32	0.750	2.61 s
	LwD	SL / Hybrid	41.13	0.913	10.0 s	34.24	0.794	2.44 s
LwD	FlowNet	RL / NC	41.17	0.915	4.00 s	34.50	0.799	0.86 s
	DiffUCO	UL / NC	41.14	0.914	2.00 s	37.48	0.868	0.46 s
	MARCO	UL / NC	42.21	0.938	2.60 s	38.87	0.900	0.42 s
	RL / NI	43.78	0.973	17.0 s	40.13	0.930	6.00 s	
	cNC <sub>greedy</sub>	RL / NC	38.96	0.866	1.70 s	30.87	0.715	1.42 s
cNC <sub>pop</sub>	cNC <sub>pop</sub>	RL / NC	39.64	0.881	1.00m	37.37	0.866	1.00m
	cNI	RL / NI	44.99	1.000	1.00m	40.28	0.933	1.00m
	PB-NCO	RL / NI+NC	<b>45.38</b>	<b>1.009</b>	1.00m	40.97	0.949	1.00m

<sup>5</sup>While the pseudocode is written sequentially for clarity, inference for all individuals is executed in parallel, and memory updates are performed in step-wise snapshots.

### A. Tackled Problems

We consider two graph-based combinatorial optimization problems within the setup of Section II-A. In both problems, an instance is  $\mathcal{I} \equiv G = (\mathcal{V}, \mathcal{E})$  (optionally with edge weights  $w_{uv} > 0$ ). Solutions are binary vectors  $\mathbf{s} \in \{0, 1\}^{|\mathcal{V}|}$ , and we maximize  $f_{\mathcal{I}}(\mathbf{s})$  over a feasible set  $\mathcal{S}(\mathcal{I})$ .

**Maximum Cut (MC)** seeks a binary labeling of nodes that places the maximum number of adjacent nodes on opposite sides; edges “cut” by the partition contribute to the score.

The feasible set is all assignments,  $\mathcal{S}_{\text{MC}}(\mathcal{I}) = \{0, 1\}^{|\mathcal{V}|}$ . The objective function weights the edges crossing the bipartition:

$$f_{\mathcal{I}}(\mathbf{s}) = \sum_{(u, v) \in \mathcal{E}} w_{uv} \mathbf{1}\{s_u \neq s_v\}, \quad \mathbf{s} \in \mathcal{S}_{\text{MC}}(\mathcal{I}) \quad (21)$$

where  $\mathbf{1}\{\cdot\}$  denotes the indicator function. Throughout the experiments we consider unweighted instances and set  $w_{uv} = 1$  for all  $(u, v) \in \mathcal{E}$ .

**Maximum Independent Set (MIS)** selects the largest subset of mutually non-adjacent nodes, so no chosen pair may share an edge. The difficulty lies in respecting feasibility while growing the set.

The feasible set enforces independence:

$$\mathcal{S}_{\text{MIS}}(\mathcal{I}) = \{\mathbf{s} \in \{0, 1\}^{|\mathcal{V}|} : \mathbf{s}_u + \mathbf{s}_v \leq 1 \ \forall (u, v) \in \mathcal{E}\}, \quad (22)$$

and the objective is to maximize the set size:

$$f_{\mathcal{I}}(\mathbf{s}) = \sum_{u \in \mathcal{V}} \mathbf{s}_u, \quad \mathbf{s} \in \mathcal{S}_{\text{MIS}}(\mathcal{I}) \quad (23)$$

Appendix A provides problem-specific implementation details for MC and MIS, including decoding procedures for cNI/cNC, reward normalization schemes, diversity metrics, and the exact feature encodings used in our experiments.

### B. Experimental Setting

**Neural Network Architecture.** We use the **Graph Transformer** (GT) [35] as the backbone encoder for both the cNI and cNC components, with lightweight multi-layer perceptrons as task-specific decoders. GT is a convenient choice because it can encode both node and edge features with high expressivity, but in principle any message-passing GNN architecture could be used. The full list of architectural hyperparameters, together with ablation studies that justify the selection, are shown in Appendix B.

**Training distributions and population setup.** For the improvement component (cNI), we train on randomly generated Erdős–Rényi (ER) graphs with edge probability 0.15 and sizes ranging from 50 to 300 nodes. For the constructive component (cNC), we train two separate policies: one on the same ER distribution, and another on RB graphs with 200–300 nodes [36]. In cNI, the shared memory is capped at  $M_{\text{max}} = 10,000$  stored solutions, and we retrieve  $k = 20$  neighbors per query using normalized Hamming distance between solution vectors. In cNC, the conditioning set is limited to  $K_{\text{max}} = 20$  reference solutions, encoded as additional feature channels, and we use the same normalized Hamming distance for the diversity term in the reward. Unless otherwise stated, we use a population

size of  $P = 20$  individuals per instance for both training and inference, and we additionally evaluate performance under varying population sizes in our ablation studies.

**Evaluation protocol.** At evaluation time, all models are applied to larger graphs without any additional training. More concretely, and following recent studies [37], [38], [39], we assess generalization on larger ER graphs (a dataset of 128 instances with 700–800 nodes) and on more challenging RB graphs [36] (a dataset of 500 instances with 800–1200 nodes).

For PB-NCO inference, we set a patience threshold of  $N_{\text{pat}} = 500$  non-improving steps before triggering a restart, and use a linear cooling schedule for the cNC exploration weight, decreasing  $\omega$  from 1.0 to 0.0 over the allocated budget. By default, populations are initialized from random feasible solutions; an alternative initialization using cNC is analyzed separately.

**Baselines.** For a more comprehensive comparison, we include exact methods using the GUROBI solver [40], simple greedy heuristics that iteratively add the item with the largest marginal gain, metaheuristics such as Genetic Algorithms (GA) [41] and Particle Swarm Optimization (PSO) [42], specialized algorithms like BURER [43] for MC and K<sub>A</sub>MIS [44] for MIS, and learning-based methods including S2V-DQN [10], ECO-DQN [7], FlowNet [39], ANYCSP [45], MARCO [20] for MC, and additionally DGL [38], LwD [37], INTEL [46] and DiffUCO [47] for MIS. Together, these methods span a broad spectrum of algorithms, including the state-of-the-art techniques. For full details on the benchmark methods, see Appendix C.

**Hardware.** Exact methods, heuristics, and metaheuristics have been executed using a cluster with 32 *Intel Xeon X5650* CPUs. Learning-based methods have been implemented using *PyTorch 2.0*, and a *Nvidia A100* GPU has been used to train the models and perform inference.

### C. Effectiveness Experiments

This section reports performance results of the proposed neural population methods on **MC** and **MIS** against the baselines listed earlier. We enforce a common *1 minute per-instance* budget to obtain compute-matched comparisons, except learning-based methods, which are run for the iteration limits recommended in the original papers. This avoids artificially inflating competing methods by giving them extra compute they were not designed to exploit. To contextualize performance across different time budgets and to enable fair comparison between constructive and iterative methods, we also report *anytime* curves (best-so-far objective vs. time).

Table I reports results on ER700–800 and RB800–1200 instances. Each cell shows the mean over five runs, the ratio to the reference objective (given by the best baseline in the row marked with \* for that setting), and the corresponding runtime. For **MC**, PB-NCO attains the best objective on both datasets, outperforming GA/PSO and the specialized BURER solver within the same budget. For **MIS**, PB-NCO achieves the best overall score on ER and, on RB, although K<sub>A</sub>MIS remains better and PB-NCO is not able to generalize as well, it is competitive with the best learning-based baselines.

Regarding the individual components, cNC in its greedy form ( $cNC_{\text{greedy}}, \omega=0$ ,  $\text{argmax}$ ) serves as an extremely fast and reasonably strong constructive heuristic; while cNC used in population mode ( $cNC_{\text{pop}}$ , sampling) and cNI on their own are able to match or surpass most learning-based competitors and classical metaheuristics.

Some methods, in particular several MIS baselines, complete in *seconds* rather than using the full one-minute budget. To provide a more fine-grained comparison across time scales, Fig. 4 shows anytime performance (best-so-far objective ratio) for PB-NCO under two initializations (Random and Constructive) together with the strongest baselines. The constructive initialization uses cNC to generate an initial population in an iterative way, treating previously built solutions as visited and increasing the exploration weight linearly from  $\omega=0$  to  $\omega=0.5$ .

Across all MC datasets and on MIS-ER, PB-NCO delivers consistently superior solution quality and maintains strong anytime behavior relative to both single-shot and iterative competitors. Constructive initialization yields better early-time performance and reaches its plateau slightly earlier, whereas random initialization starts weaker but catches up over longer budgets; by the end of the run both variants are nearly indistinguishable. Variability is very low overall and slightly smaller for random initialization (ratio standard deviation of order  $10^{-4}$  at 60s in MC), indicating stable behavior across runs.

Figure 5 contrasts PB-NCO with population-based metaheuristics (GA and PSO) using the same population size, operators, and time budget. PB-NCO converges faster and to higher-quality solutions in both MC and MIS, highlighting the benefits of the neural population framework over classical population metaheuristics.

#### D. Diversity Study

We analyze diversity in the setting where a distance signal is most natural: the cNC policy. We compare cNC with different exploration weights  $\omega$  to a baseline policy with the *same* network but trained without any conditioning set (NC baseline, i.e., no diversity-aware learning). Both methods start from the same initial population of random solutions; we then generate one additional solution at a time and, after each step, compute the mean pairwise Hamming distance (normalized by problem size) over the *entire* history of visited solutions. Figure 6 shows that all procedures begin from the same random initial diversity, but the baseline quickly collapses: as more solutions are generated, it concentrates on a narrow region of the search space and the historical diversity drops steadily. In contrast, cNC maintains substantially higher diversity throughout the run for a wide range of  $\omega$  values.

A natural question is why we do not apply the same distance-based diversity reward in the cNI component. In an improvement setting, cNI performs local moves in the neighborhood of the current solution; enforcing large distances at every step would push the policy to undo recent improvements, which conflicts with the role of local search. For this reason, we use cNI’s repetition penalty primarily to avoid exact revisits, and reserve distance-based diversity shaping for

the cNC component, where new solutions can be instantiated anywhere in the search space.

#### E. Ablation Study

In this section we quantify the contribution of PB-NCO’s core components via controlled ablations. Unless stated otherwise, all variants use the same training protocol, seeds, population size (20 individuals), and a larger time budget of 5 minutes.

- *Level 1 + Mem.*. Disables the centralized shared memory both during training and inference. Individuals keep private memories and never read/write across population. This is the equivalent to a Level 1 method mentioned in Section III, but with a memory module to avoid repetitions. The restart policy, when triggered, conditions only on the focal trajectory’s own history. This isolates the contribution of population-level communication and coordination via the shared memory.
- *cNI*. We include the Level 2 proposal with shared memory but without restarts.
- *Random-Restarts*. Preserves the cNI and the restart scheduler, but replaces the cNC initializer with random restarts drawn from the problem’s native sampling scheme. This isolates the value of the learned constructive policy.

TABLE II  
ABLATION EXPERIMENT. PERFORMANCE COMPARISON ON MC AND MIS PROBLEMS FOR DIFFERENT ABLATION SETTINGS.

	Method	ER700-800			RB800-1200		
		Obj. $\uparrow$	Ratio $\uparrow$	Time	Obj. $\uparrow$	Ratio $\uparrow$	Time
MC	Level 1 + Mem.	24230.26	1.000	5.00m	31545.68	1.000	5.00m
	cNI	24232.17	1.000	5.00m	31545.97	1.000	5.00m
	Random-Restarts	24269.50	1.001	5.00m	31547.60	1.000	5.00m
	PB-NCO	<b>24275.17</b>	<b>1.002</b>	5.00m	<b>31548.03</b>	<b>1.000</b>	5.00m
MIS	Level 1 + Mem.	45.12	1.003	5.00m	40.40	0.936	5.00m
	cNI	45.19	1.004	5.00m	40.67	0.942	5.00m
	Random-Restarts	45.29	1.006	5.00m	40.75	0.944	5.00m
	PB-NCO	<b>45.44</b>	<b>1.010</b>	5.00m	<b>41.44</b>	<b>0.960</b>	5.00m

Table II summarizes the ablation results, reporting (i) objective value, (ii) ratio to the strongest baseline for each dataset, and (iii) runtime. Across problems and datasets, all three variants underperform the full PB-NCO, confirming that shared memory, learned constructive restarts, and the restart scheduler each contribute to performance.

A notable observation concerns the per-individual mean objective. The *Level 1 + Mem.* variant exhibits a higher average across the 20 individuals than PB-NCO, yet its elite (best-of-population) solution is consistently worse. This is expected: PB-NCO deliberately spreads the population via memory-conditioned coordination and restarts, allocating some individuals to intensify around promising regions while others probe diverse areas. Interestingly, we have seen that the resulting higher inter-individual variance lowers the average objective value of the individuals but raises the maximum, precisely the quantity that matters in population-based search.

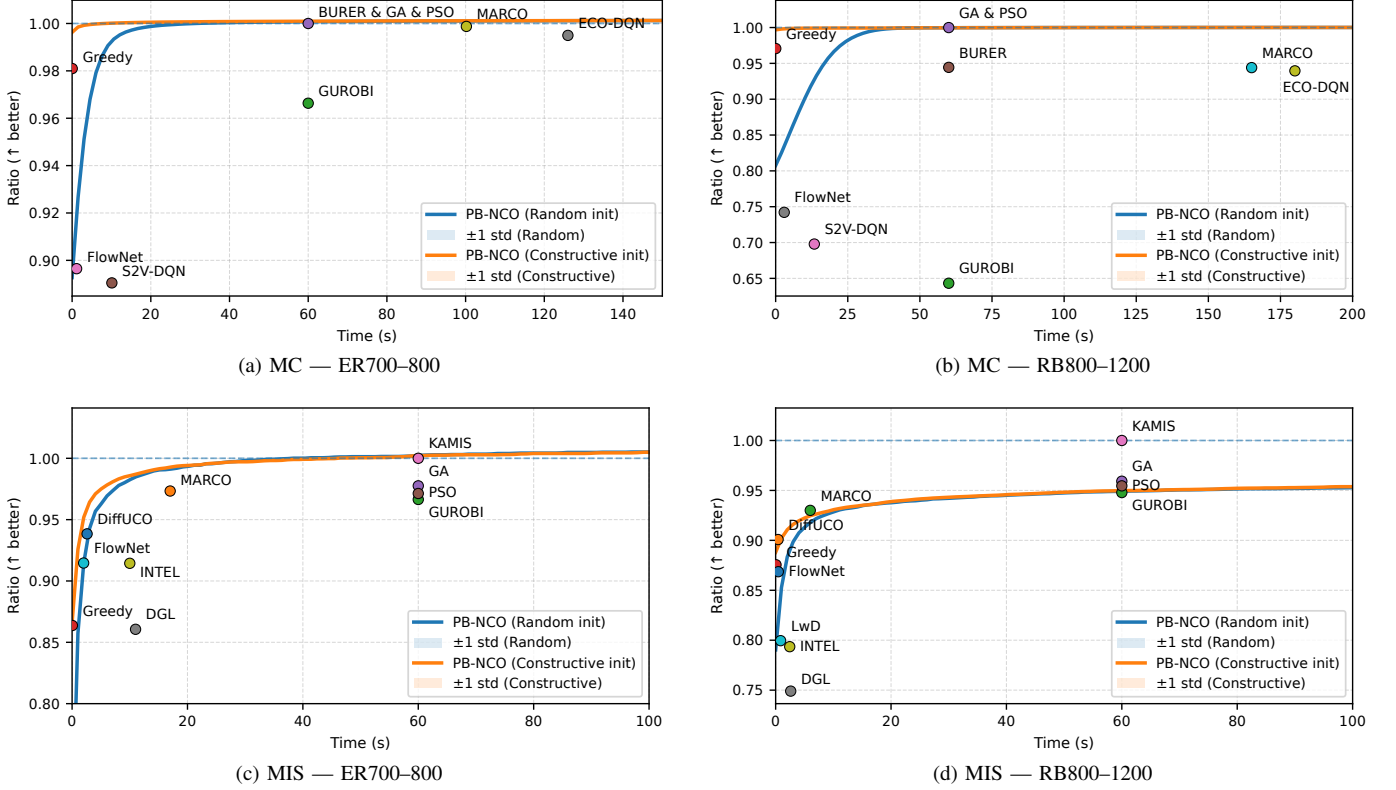


Fig. 4. Anytime performance against baselines. Solid lines denote the average best-so-far ratio (current objective / reference objective); shaded bands denote the standard deviation over five runs. Results are shown for both MC and MIS in ER700-800 and RB800-1200 graphs.

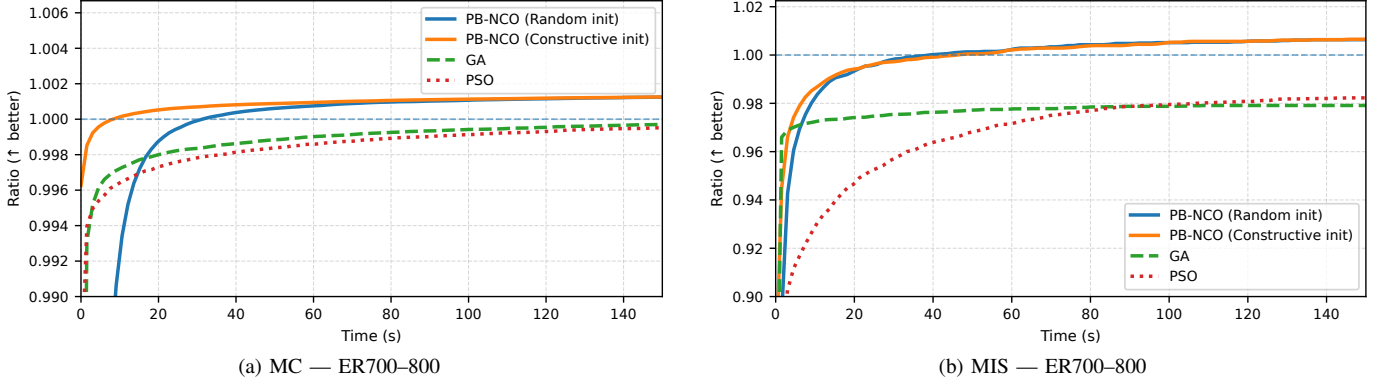


Fig. 5. Anytime performance against metaheuristics. Solid lines denote the average best-so-far ratio (current objective / reference objective); shaded bands denote the standard deviation over five runs. Results are shown for both MC and MIS in ER700-800 graphs.

## F. Hyperparameter Sensitivity Analysis

Beyond the main ablations, we examine sensitivity to three hyperparameters that affect performance: population size, restart patience (the number of non-improving steps before triggering a restart), and different strategies to select the conditioning set for the cNC policy.

**Population Size.** We present the results of various population sizes under the same time budget in Fig. 7. As expected, smaller populations improve faster at the beginning because, under a fixed time budget, the algorithm completes more iterations of improvement per candidate, so good solutions appear sooner. After the initial improvement phase, the curves

begin to flatten: in our experiments, populations of  $N \geq 5$  achieve very similar final performance, suggesting diminishing returns beyond a small but non-trivial population. In contrast, the run with  $N = 1$ , which cannot exploit population-level mechanisms, is consistently worse at the end of the execution.

Overall, we observe clear diminishing returns with large population sizes: diversity helps, but beyond a moderate range it no longer translates into much better final performance, while the time to process the same fixed work budget increases linearly with population size, as shown in Fig. 8.

**Restarting Patience.** We study the restart patience  $N_{\text{pat}}$ , the number of consecutive non-improving iterations an individual is allowed before restart, on ER700–800 with  $N_{\text{pat}} \in$

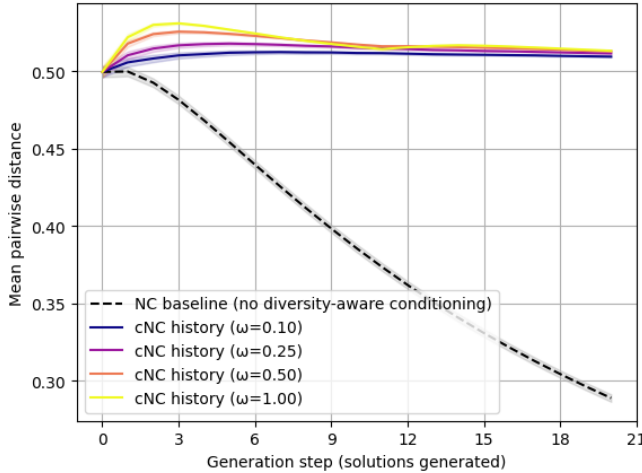


Fig. 6. **Diversity during cNC search.** Mean pairwise normalized Hamming distance over all solutions visited so far, for the NC baseline (no diversity-aware conditioning) and for cNC with several exploration weights  $\omega$ .

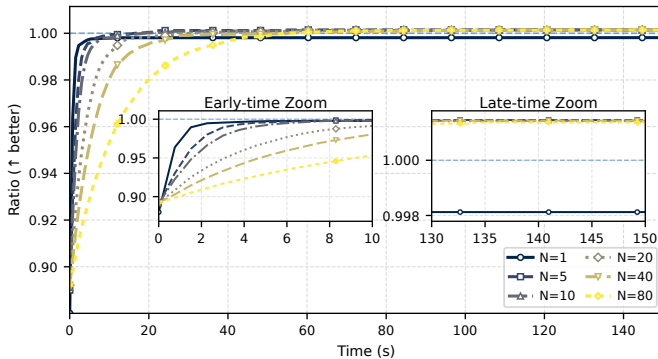


Fig. 7. **Population Size.** Anytime performance vs. population size for ER700-800 graphs in the MC problem.

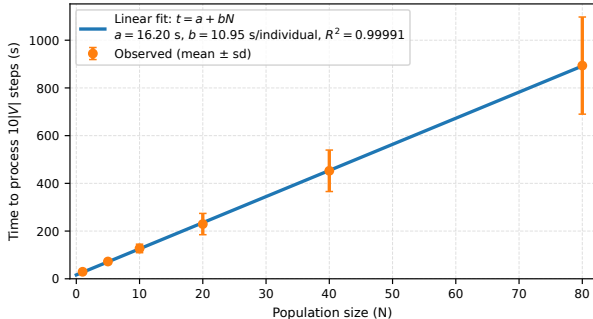


Fig. 8. Time to process  $10|V|$  environment steps (7000-8000 for ER700-800) as a function of population size  $N$ . Markers show mean  $\pm$  s.d. across runs; the solid line is a linear fit  $t = a + bN$  with  $a \approx 16.2$  s and  $b \approx 10.95$  s/individual ( $R^2 \approx 0.99991$ ), indicating near-linear scaling with a small fixed overhead.

$\{100, 500, 1000, 5000\}$ . A low value can cause premature exploration, potentially missing out on good solutions, while a high value can result in excessive computation within a local region of the search space without yielding significant improvements.

In our runs, moderate settings performed best: for MC-ER,  $N_{\text{pat}}=500$  and 1000 produced nearly identical top results ( $\approx 24266$ ), whereas both 100 and 5000 were consistently lower

( $\approx 24254$  and  $\approx 24256$ ). MIS-ER showed the same ordering ( $\approx 45.38/45.37$  at 500/1000 vs.  $\approx 45.11/45.19$  at 100/5000). Based on these observations, setting the patience to the number of nodes in the graph instance ( $N_{\text{pat}} \approx |\mathcal{V}|$ ) serves as a simple yet effective rule of thumb.

**Conditioning Set Selection Strategy.** Recall that restarts condition the constructor on a set  $\mathcal{K}_t = \text{SelectK}(\mathcal{M}_t)$  drawn from the memory  $\mathcal{M}_t$ , asking it to propose seeds that are *dissimilar* to  $\mathcal{K}_t$ . With population size  $P=20$  and  $k=20$ , we compare three instantiations of SelectK: (i)  $\text{SelectK}_{\text{last}}$ : the last  $k$  insertions into  $\mathcal{M}_t$  made by the *whole population*; (ii)  $\text{SelectK}_{\text{best-global}}$ : one best-so-far solution per individual ( $P$  items; here  $k = P$ ); (iii)  $\text{SelectK}_{\text{best-current}}$ : one local-best since the last restart per individual. Results show that  $\text{SelectK}_{\text{last}}$  yields the best late-time plateaus, closely followed by  $\text{SelectK}_{\text{best-global}}$ .  $\text{SelectK}_{\text{best-current}}$  underperforms throughout.

**Other hyperparameters.** In our experiments, the memory capacity had no practical effect: for runs up to 5 minutes on graphs with up to 1200 nodes, the limit  $M_{\text{max}}$  was never reached. We also varied the number of neighbors  $k$  in the  $k$ NN memory retrieval and did not observe any significant difference for  $k > 5$ , so we fixed  $k = 20$ , equal to the default population size. Regarding the distance metric, we tested edge-based Hamming distance and Jaccard coverage (for MIS), but found that node-level Hamming distance performed best on both MC and MIS, and used it throughout the experiments.

## G. Training the Conditioned Neural Constructive

We now analyze the behavior of the cNC policy from a bi-objective perspective. Here we consider cNC in its single-pass greedy form (one construction per call, without the population loop), and study how it trades off solution quality and distance to a conditioning set through the exploration weight  $\omega$  (see Sec. IV-B). We focus on two questions: (i) whether a single conditioned policy can replace a bank of specialized policies trained for fixed trade-offs, and (ii) how the sampling scheme for  $\omega$  during training affects the quality of the learned Pareto front.

**Conditioned network vs. bank of independent networks.** We compare a single conditioned policy  $\pi_\theta(\cdot | \omega)$  to a bank of independent policies  $\{\pi_{\theta_\omega}\}$ , each trained for a fixed weight  $\omega \in \{0.0, 0.1, \dots, 1.0\}$ . Figure 9 plots, for varying exploration weights  $\omega$ , the achieved solution quality (y-axis) against the exploration reward given as the average pairwise distance over solutions (x-axis).

The conditioned model traces out a Pareto set that dominates a large fraction of the per- $\omega$  specialists, while using a single parameter vector (lower training and storage cost) and providing continuous control at inference (any  $\omega$ , not just the training grid). This suggests that, rather than overfitting to a single scalarization, training in multiple scenarios helps discover policies that generalize better.

**Sampling the exploration weight during training.** A natural question is how to sample  $\omega$  during training so that the learned policy approximates the Pareto front effectively. Rather than drawing  $\omega \sim \mathcal{U}[0, 1]$  for each episode, we

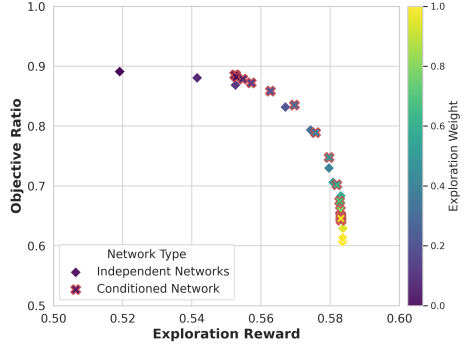


Fig. 9. Independently trained networks and the conditioned network deployed with different weights.

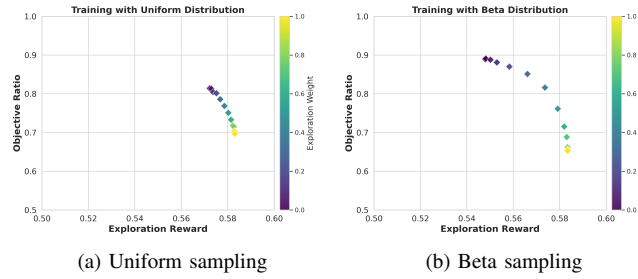


Fig. 10. Effect of training-time exploration-weight sampling on the learned quality–diversity trade-off. Comparison of the conditioned neural constructive (cNC) trained with uniform sampling  $\omega \sim \mathcal{U}[0, 1]$  versus Beta(0.2, 0.2) sampling.

found that biasing  $\omega$  toward the extremes leads to a better approximation of the *boundary* of the front. Concretely, we sample  $\omega \sim \text{Beta}(\alpha, \beta)$  with  $\alpha = \beta = 0.2$ , which concentrates probability mass near 0 (pure intensification) and 1 (pure diversification). Figure 10 contrasts the fronts obtained with uniform versus Beta sampling and shows a clear improvement near the extremes when using the latter.

We found that moderate concentration near the boundaries works best:  $\alpha = \beta \in [0.1, 0.2]$  gives good interior coverage while still emphasizing the extremes. Larger values behave too much like the uniform case, and very small values over-focus on extremes, making intermediate trade-offs harder to learn.

## VI. LIMITATIONS AND OPPORTUNITIES.

The proposed methods show that neural constructive and improvement operators can be combined into efficient population-based search procedures through shared memory, conditioning, and restart mechanisms. At the same time, our implementations are intentionally simple, and they expose a number of practical limitations that are likely to matter as problem size, run length, and population size increase. This section summarizes the main constraints observed or implied by our design choices, and outlines clear opportunities to improve scalability, better exploit population information, and replace hand-crafted control rules with more adaptive mechanisms.

**cNI.** Our cNI implementation relies on an explicit memory that stores many visited solutions. For very long runs and large

populations, keeping all candidates can become prohibitive. Scalable variants, such as storing only cluster representatives in solution space or applying more aggressive, diversity-aware pruning rules, could preserve coverage of the search space while keeping memory bounded. Moreover, cNI currently queries memory using a fixed distance function  $d(\cdot, \cdot)$  and a weighted average of the  $k$  nearest neighbors. An interesting extension would be to *learn* the retrieval mechanism itself: for example, training an encoder that maps solutions to a latent space where  $k$ -NN is more informative, and learning attention weights over retrieved neighbors instead of using linear distance decay.

**cNC.** The current cNC policy conditions on a fixed-size subset of solutions, encoded as at most  $K_{\max}$  additional feature channels. This is sufficient for our purposes, but it inevitably truncates the search history, imposes an arbitrary ordering on the conditioning set (the encoding is not permutation-invariant), and restricts the population structure the model can exploit. A natural line of work is to move toward richer Level 3 conditioning mechanisms: for instance, attending over a compact set of learned memory embeddings rather than raw solutions, using graph encoders that handle variable-size conditioning sets in a permutation-invariant way, or introducing hierarchical memories that summarize different regions of the search space.

**PB-NCO.** Our PB-NCO implementation uses a simple patience-based rule to trigger cNC restarts and a hand-crafted schedule for the exploration weight  $\omega$ . This mechanism is effective but inherently myopic: it treats all trajectories symmetrically, even though some are more promising to continue than others, and it does not explicitly account for how restarts influence global population diversity. A natural extension is to replace these rules with adaptive controllers, for example a small learned policy that decides which trajectories to restart based on their recent progress and novelty.

**Architectural and training heterogeneity.** All three components rely on a single shared policy trained on a fixed instance distribution. In practice, population-based methods often benefit from heterogeneity, with different individuals playing distinct roles. A natural next step is to consider populations of role-conditioned policies tackling the same instance, allowing different policies to specialize on complementary behaviors and thereby exploiting this additional source of diversity.

## VII. CONCLUSION

Motivated by the lack of neural counterparts to population metaheuristics, this work shows that explicitly modeling population structure can substantially improve neural combinatorial optimization. Coordinating many trajectories via shared-memory interaction and memory-conditioned restarts consistently improves solution quality while sustaining diversity compared with non-coordinated baselines. Although population-level coordination introduces additional components and design choices, the empirical gains suggest that learning how candidates interact is a promising direction. We hope this work motivates further research on neural population

mechanisms, including alternative communication topologies, diversity preservation objectives, and scalable memory designs. To support reproducible comparison and follow-up work, we release code and evaluation pipelines<sup>6</sup>.

## APPENDIX A PROBLEM-SPECIFIC IMPLEMENTATION DETAILS

### A. Maximum Cut (MC)

**cNC Decoding.** For MC, cNC is implemented in one shot: the network outputs a probability  $\pi_u \in [0, 1]$  for each node  $u$  to belong to one side of the cut, and a full solution is obtained by sampling all nodes in a single forward pass (without  $O(|\mathcal{V}|)$  autoregressive decoding).

**Symmetry.** To break the global symmetry (flipping all bits leaves the cut value unchanged), we fix the label of a reference node to 1 and give it a small dedicated embedding, so the model has a canonical side of the partition.

**Reward.** Given graph instance  $\mathcal{I}$  with nodes  $\mathcal{V}$  and edges  $\mathcal{E}$ , the RL reward is the centered, rescaled value  $\tilde{f}_{\mathcal{I}}(\mathbf{s}) = (f_{\mathcal{I}}(\mathbf{s}) - \text{baseline}(\mathcal{I})) / \text{scale}(\mathcal{I})$ , where the baseline is the expected cut of a random bi-partition:  $\text{baseline}(\mathcal{I}) = |\mathcal{E}|/2$ , and the scale is in a typical deviation of a very good cut above the random baseline:

$$\text{scale}(\mathcal{I}) = \sqrt{\frac{|\mathcal{E}| |\mathcal{V}| \log 2}{2}}.$$

**Distance and random solutions.** For diversity, both memory retrieval and cNC’s diversity reward use normalized Hamming distance. Random initial solutions are generated by assigning each node to one side of the partition independently with probability 1/2.

### B. Maximum Independent Set (MIS)

**Feasible decoding in cNC and cNI.** For MIS, some solutions are infeasible (unlike MC), so both constructive and improvement policies must enforce independence. In cNC, the model produces a single vector of inclusion scores over all nodes. These scores are computed in one forward pass, then sorted, and nodes are processed greedily in that order: a node is activated only if it is not adjacent to any previously selected node. Thus, feasibility is enforced by a sequential post-processing step. In cNI, feasibility is handled directly in the action space by masking out all moves that would violate independence (e.g., turning on a node adjacent to an active one), so every local move keeps the solution feasible.

**Reward.** Let  $L(\mathcal{I})$  be the Caro-Wei lower surrogate [48] and  $U(\mathcal{I})$  an upper surrogate based on a greedy maximal matching for instance  $\mathcal{I}$ . Given a raw MIS value  $f_{\mathcal{I}}(\mathbf{s})$ , we normalize the reward as

$$\tilde{f}_{\mathcal{I}}(\mathbf{s}) = \frac{f_{\mathcal{I}}(\mathbf{s}) - L(\mathcal{I})}{U(\mathcal{I}) - L(\mathcal{I})}. \quad (24)$$

Concretely,

$$L(\mathcal{I}) = \sum_{v \in V} \frac{1}{\deg(v) + 1}, \quad U(\mathcal{I}) = N - \text{match}(\mathcal{I}), \quad (25)$$

<sup>6</sup>Code will be released upon paper acceptance.

where  $\deg(v)$  is the degree of node  $v$ ,  $N = |\mathcal{V}|$ , and  $\text{match}(\mathcal{I})$  is the size of a greedy maximal matching.

**Distance and random solutions.** As in MC, diversity and memory retrieval use normalized Hamming distance on the  $\{0, 1\}^{|\mathcal{V}|}$  indicator vectors. Random solutions are generated by a randomized greedy heuristic: nodes are chosen uniformly at random from the remaining candidates, added to the set, and their neighbors are removed until no candidates remain.

### C. Feature Encoding

In all cases we encode the graph through edge features derived from the adjacency, and node features that combine solution and population information.

**cNI.** The following node features are used: (i) a binary feature for the current solution, and (ii) a dense feature from memory: we retrieve the  $k$  nearest neighbors in memory (normalized Hamming distance) and take a distance-weighted average of their indicator vectors, as in [20]. This aggregated vector is added as an extra node channel.

**cNC.** Nodes carry: (i) one binary channel per reference solution in the conditioning set  $\mathcal{K}$  (up to  $K_{\max}$  channels), and (ii) a scalar feature with the exploration weight  $\omega$ , broadcast to all nodes.

## APPENDIX B NEURAL NETWORK HYPERPARAMETER SELECTION

TABLE III  
SELECTED MODEL HYPERPARAMETERS

Model Hyperparameter	Value
Number of layers ( $L$ )	3
Hidden dimension ( $d$ )	64
Number of heads ( $h$ )	8
FFNN hidden dimension	256
Activation function	GeLU
Normalization	LayerNorm
Dropout	0%

TABLE IV  
PERFORMANCE UNDER VARIATIONS FROM THE USED HYPERPARAMETER SETTING. WE REPORT THE AVERAGE OBJECTIVE VALUE OBTAINED WHEN TESTING THE NI MODEL AFTER THE LAST EPOCH OF TRAINING ON ER GRAPH INSTANCES WITH 20, 60, 100 AND 200 NODES FOR THE MC PROBLEM.

Setting	ER60	ER100	ER200
<b>Used Config:</b> $L = 3$ , $d = 64$ , LayerNorm, Dropout 0%	192.7	503.6	1896.9
<b>Number of Layers</b>			
$L = 2$	192.4	502.1	1856.7
$L = 4$	192.6	503.2	1881.4
<b>Hidden Dimension</b>			
$d = 128$	192.6	502.7	1885.6
<b>Normalization</b>			
Instance	192.7	503.4	1894.6
RMS	192.6	503.2	1892.3
<b>Dropout</b>			
Dropout = 20%	192.7	503.2	1887.6

Table III lists the hyperparameters used in the GT model. These were determined through a comprehensive hyperparameter study, where different NI models were trained for 10,000 episodes on instances ranging from 20 to 40 nodes, and using a batch size of 1024. We explored various hyperparameter configurations and present the performance results on 100 instances with sizes of 60, 100, and 200 nodes in Table IV.

## APPENDIX C

### IMPLEMENTATION DETAILS OF BASELINE METHODS

In this section, we provide a more detailed description of the methods used in the experiments.

a) *Maximum Cut*.: For the MC problem, we used the methods implemented in the Max Cut Benchmark [49], modifying them to incorporate a time limit as a stopping criterion. Specifically, we employed the GUROBI exact solver [40] which is not able to obtain optimal solutions in the given budget, but provides an approximate solution. We also used constructive heuristics such as Forward Greedy, which starts with an empty solution and iteratively adds the vertex that provides the largest gain in the objective value. We applied metaheuristic techniques including Tabu Search (TS) [50], which maintains a tabu list to avoid revisiting recently explored solutions. The benchmark also includes learning-based methods, including S2V-DQN [10], a NC method guided by a GNN; ECO-DQN [7], a Neural Improvement variant of S2V-DQN; FlowNet [39], a work that samples from the solution space with Generative Flow Networks; and ANYCSP [45], a GNN-based search method for any constraint satisfaction problem.

Additionally, we integrated a Genetic Algorithm (GA) [41], a population-based metaheuristic that evolves solutions through selection, crossover, and mutation operations; Particle Swarm Optimization (PSO) [42], a swarm-based optimization technique where a population of candidate solutions, called particles, moves through the solution space guided by individual and collective experiences; BURER [43], a specialized algorithm for MC that leverages semidefinite programming relaxations to approximate solutions; and MARCO [20], a memory-based NCO method that uses a shared memory to guide the search to unvisited solutions.

b) *Maximum Independent Set*: We reused several methods also for MIS. We employed the GUROBI exact solver, a greedy constructive heuristic that iteratively adds the node maximizing the gain while ensuring feasibility to the MIS constraints. We also implemented a Genetic Algorithm, a PSO, and used the MIS implementations of FlowNet and MARCO.

Apart from these benchmark methods, we included KAMIS [44], an evolutionary approach that combines graph kernelization, local search, and graph partitioning techniques to solve the MIS problem. Furthermore, we integrated several learning-based methods: DGL [38] and INTEL [46], which combine a policy learnt by supervised learning with tree search; LwD [37], a scalable reinforcement learning framework that adaptively defers element-wise decisions during solution generation to simplify hard decisions; and DiffUCO [47], a diffusion model using unsupervised learning to

approximate intractable discrete distributions without requiring training data.

## ACKNOWLEDGMENT

This work was supported by the University of the Basque Country (project US24/22), and Spanish Ministry of Science, Innovation and Universities (project PID2023-149195NB-I00).

## REFERENCES

- [1] Y. Bengio, A. Lodi, and A. Prouvost, “Machine learning for combinatorial optimization: a methodological tour d’horizon,” *European Journal of Operational Research*, vol. 290, no. 2, pp. 405–421, 2021.
- [2] N. Mazyavkina, S. Sviridov, S. Ivanov, and E. Burnaev, “Reinforcement learning for combinatorial optimization: A survey,” *Computers & Operations Research*, vol. 134, p. 105400, 2021.
- [3] I. Bello, H. Pham, Q. V. Le, M. Norouzi, and S. Bengio, “Neural combinatorial optimization with reinforcement learning,” *arXiv preprint arXiv:1611.09940*, 2016.
- [4] W. Kool, H. van Hoof, and M. Welling, “Attention, learn to solve routing problems!” in *International Conference on Learning Representations*, 2018.
- [5] R. Wang, J. Yan, and X. Yang, “Neural graph matching network: Learning lawler’s quadratic assignment problem with extension to hypergraph and multiple-graph matching,” *IEEE Transactions on Pattern Analysis and Machine Intelligence*, vol. 44, no. 9, pp. 5261–5279, 2021.
- [6] C. Zhang, W. Song, Z. Cao, J. Zhang, P. S. Tan, and X. Chi, “Learning to dispatch for job shop scheduling via deep reinforcement learning,” *Advances in neural information processing systems*, vol. 33, pp. 1621–1632, 2020.
- [7] T. Barrett, W. Clements, J. Foerster, and A. Lvovsky, “Exploratory combinatorial optimization with reinforcement learning,” in *Proceedings of the AAAI conference on artificial intelligence*, vol. 34, 2020, pp. 3243–3250.
- [8] C. Blum and A. Roli, “Metaheuristics in combinatorial optimization: Overview and conceptual comparison,” *ACM computing surveys (CSUR)*, vol. 35, no. 3, pp. 268–308, 2003.
- [9] S. Liu, Y. Zhang, K. Tang, and X. Yao, “How good is neural combinatorial optimization? a systematic evaluation on the traveling salesman problem,” *IEEE Computational Intelligence Magazine*, vol. 18, no. 3, pp. 14–28, 2023.
- [10] E. Khalil, H. Dai, Y. Zhang, B. Dilkina, and L. Song, “Learning combinatorial optimization algorithms over graphs,” *Advances in neural information processing systems*, vol. 30, 2017.
- [11] Y.-D. Kwon, J. Choo, B. Kim, I. Yoon, Y. Gwon, and S. Min, “Pomo: Policy optimization with multiple optima for reinforcement learning,” *Advances in Neural Information Processing Systems*, vol. 33, pp. 21 188–21 198, 2020.
- [12] F. Luo, X. Lin, Z. Wang, X. Tong, M. Yuan, and Q. Zhang, “Self-improved learning for scalable neural combinatorial optimization,” *arXiv preprint arXiv:2403.19561*, 2024.
- [13] Q. Cappart, D. Chételat, E. B. Khalil, A. Lodi, C. Morris, and P. Veličković, “Combinatorial optimization and reasoning with graph neural networks,” *Journal of Machine Learning Research*, vol. 24, no. 130, pp. 1–61, 2023.
- [14] C. Zhou, X. Lin, Z. Wang, X. Tong, M. Yuan, and Q. Zhang, “Instance-conditioned adaptation for large-scale generalization of neural combinatorial optimization,” *arXiv preprint arXiv:2405.01906*, 2024.
- [15] O. Vinyals, M. Fortunato, and N. Jaitly, “Pointer networks,” *Advances in neural information processing systems*, vol. 28, 2015.
- [16] X. Chen and Y. Tian, “Learning to perform local rewriting for combinatorial optimization,” *Advances in Neural Information Processing Systems*, vol. 32, 2019.
- [17] H. Lu, X. Zhang, and S. Yang, “A learning-based iterative method for solving vehicle routing problems,” in *International conference on learning representations*, 2019.
- [18] Y. Wu, W. Song, Z. Cao, J. Zhang, and A. Lim, “Learning improvement heuristics for solving routing problems,” *IEEE transactions on neural networks and learning systems*, vol. 33, no. 9, pp. 5057–5069, 2021.
- [19] T. D. Barrett, C. W. Parsonson, and A. Laterre, “Learning to solve combinatorial graph partitioning problems via efficient exploration,” *arXiv preprint arXiv:2205.14105*, 2022.

[20] A. I. Garmendia, Q. Cappart, J. Ceberio, and A. Mendiburu, “Marco: a memory-augmented reinforcement framework for combinatorial optimization,” in *Proceedings of the Thirty-Third International Joint Conference on Artificial Intelligence*, 2024, pp. 6931–6939.

[21] F. Chalumeau, R. Shabe, N. De Nicola, A. Pretorius, T. D. Barrett, and N. Grinsztajn, “Memory-enhanced neural solvers for efficient adaptation in combinatorial optimization,” *arXiv preprint arXiv:2406.16424*, 2024.

[22] H. Liu, Z. Zong, Y. Li, and D. Jin, “Neurocrossover: An intelligent genetic locus selection scheme for genetic algorithm using reinforcement learning,” *Applied Soft Computing*, vol. 146, p. 110680, 2023.

[23] I. Greenberg, P. Sielski, H. Linsenmaier, R. Gandham, S. Mannor, A. Fender, G. Chechik, and E. Meirom, “Accelerating vehicle routing via ai-initialized genetic algorithms,” *arXiv preprint arXiv:2504.06126*, 2025.

[24] H. Ye, J. Wang, Z. Cao, H. Liang, and Y. Li, “Deepaco: neural-enhanced ant systems for combinatorial optimization,” *Advances in Neural Information Processing Systems*, vol. 36, 2024.

[25] M. Dorigo and T. Stützle, *Ant colony optimization: overview and recent advances*. Springer, 2019.

[26] N. Grinsztajn, D. Furelos-Blanco, S. Surana, C. Bonnet, and T. Barrett, “Winner takes it all: Training performant rl populations for combinatorial optimization,” *Advances in Neural Information Processing Systems*, vol. 36, pp. 48485–48509, 2023.

[27] A. Hottung, M. Mahajan, and K. Tierney, “Polynet: Learning diverse solution strategies for neural combinatorial optimization,” *arXiv preprint arXiv:2402.14048*, 2024.

[28] T. Vidal, T. G. Crainic, M. Gendreau, and C. Prins, “A unified solution framework for multi-attribute vehicle routing problems,” *European Journal of Operational Research*, vol. 234, no. 3, pp. 658–673, 2014.

[29] F. Luo, X. Lin, F. Liu, Q. Zhang, and Z. Wang, “Neural combinatorial optimization with heavy decoder: Toward large scale generalization,” *Advances in Neural Information Processing Systems*, vol. 36, pp. 8845–8864, 2023.

[30] I. Dunning, S. Gupta, and J. Silberholz, “What works best when? a systematic evaluation of heuristics for max-cut and qubo,” *INFORMS Journal on Computing*, vol. 30, no. 3, pp. 608–624, 2018.

[31] E. L. Lawler, J. K. Lenstra, and A. Rinnooy Kan, “Generating all maximal independent sets: Np-hardness and polynomial-time algorithms,” *SIAM Journal on Computing*, vol. 9, no. 3, pp. 558–565, 1980.

[32] R. S. Sutton and A. G. Barto, *Reinforcement learning: An introduction*. MIT press, 2018.

[33] A. Abels, D. Roijers, T. Lenaerts, A. Nowé, and D. Steckelmacher, “Dynamic weights in multi-objective deep reinforcement learning,” in *International conference on machine learning*. PMLR, 2019, pp. 11–20.

[34] F. Felten, E.-G. Talbi, and G. Danoy, “Multi-objective reinforcement learning based on decomposition: A taxonomy and framework,” *Journal of Artificial Intelligence Research*, vol. 79, pp. 679–723, 2024.

[35] V. P. Dwivedi and X. Bresson, “A generalization of transformer networks to graphs,” *arXiv preprint arXiv:2012.09699*, 2020.

[36] K. Xu and W. Li, “Exact phase transitions in random constraint satisfaction problems,” *Journal of Artificial Intelligence Research*, vol. 12, pp. 93–103, 2000.

[37] S. Ahn, Y. Seo, and J. Shin, “Learning what to defer for maximum independent sets,” in *International conference on machine learning*. PMLR, 2020, pp. 134–144.

[38] M. Böther, O. Kifbig, M. Taraz, S. Cohen, K. Seidel, and T. Friedrich, “What’s wrong with deep learning in tree search for combinatorial optimization,” in *International Conference on Learning Representations*, 2021.

[39] D. Zhang, H. Dai, N. Malkin, A. Courville, Y. Bengio, and L. Pan, “Let the flows tell: Solving graph combinatorial problems with gflownets,” in *Thirty-seventh Conference on Neural Information Processing Systems*, 2023.

[40] Gurobi Optimization, LLC, “Gurobi Optimizer Reference Manual,” 2023. [Online]. Available: <https://www.gurobi.com>

[41] O. Kramer and O. Kramer, *Genetic algorithms*. Springer, 2017.

[42] J. Kennedy and R. Eberhart, “Particle swarm optimization,” in *Proceedings of ICNN’95-international conference on neural networks*, vol. 4. ieee, 1995, pp. 1942–1948.

[43] S. Burer, R. D. Monteiro, and Y. Zhang, “Rank-two relaxation heuristics for max-cut and other binary quadratic programs,” *SIAM Journal on Optimization*, vol. 12, no. 2, pp. 503–521, 2002.

[44] S. Lamm, P. Sanders, C. Schulz, D. Strash, and R. F. Werneck, “Finding near-optimal independent sets at scale,” in *2016 Proceedings of the Eighteenth Workshop on Algorithm Engineering and Experiments (ALENEX)*. SIAM, 2016, pp. 138–150.

[45] J. Tönshoff, B. Kisin, J. Lindner, and M. Grohe, “One model, any csp: graph neural networks as fast global search heuristics for constraint satisfaction,” in *Proceedings of the Thirty-Second International Joint Conference on Artificial Intelligence*, 2023, pp. 4280–4288.

[46] Z. Li, Q. Chen, and V. Koltun, “Combinatorial optimization with graph convolutional networks and guided tree search,” *Advances in neural information processing systems*, vol. 31, 2018.

[47] S. Sanokowski, S. Hochreiter, and S. Lehner, “A diffusion model framework for unsupervised neural combinatorial optimization,” *arXiv preprint arXiv:2406.01661*, 2024.

[48] S. M. Selkow, “A probabilistic lower bound on the independence number of graphs,” *Discrete Mathematics*, vol. 132, no. 1-3, pp. 363–365, 1994.

[49] A. Nath and A. Kuhnle, “A benchmark for maximum cut: Towards standardization of the evaluation of learned heuristics for combinatorial optimization,” *arXiv preprint arXiv:2406.11897*, 2024.

[50] F. Glover, “Tabu search: A tutorial,” *Interfaces*, vol. 20, no. 4, pp. 74–94, 1990.